Stress and frequency analysis of the evaporator new pigtails design – Revision A

Author:
Antonio Alvino

Prepared For:
INFN Perugia
AMS-02 – TTCS Collaboration

Report Created:
Monday, May 15, 2006

Report Last Modified:
Sunday, July 09, 2006

Software Used:
ANSYS 9.0

Database:
D:\LAVORO\Pig Tails redesign\PIG TAILS FEM\ spirale con vincoli (19 MAGGIO).wbdb

Contents

1. Purpose

The purpose of this report is both to update the structural analysis of the evaporator assembly made by Mr. B.Verlaat and C.Snippe (issued in February,18 2005) by using the new design and to add other loads which the tubes will have to undergo during the launch.

A more accurate knowledge of the static and dynamic behaviour of the object is useful in order to discover and correct critical points of the design before to manufacture it.

In the following simulations, the loads (VC flange deflection, Launch accelerations and internal pressure) have been applied both independently (see paragraphs 2.3 – 2.4 – 2.5) and simultaneously (see paragraph 2.6).

Based on the analysis results, it turned out that the VC flange deflection is the most critical load. It's not totally clear yet whether 10mm is the maximum flange deflection or deflection which takes place on the bracket location.

Then, the effect of several VC deflections (combined both with the internal pressure and with launch loads) have been investigated in paragraph 2.6.2.

Tab. 14 shows that the max VC flange deflection allowed is lower than about 6 mm. If that wouldn't be enough, a design solution could be to clasp the tubes in a more external zone of the flange in which VC deflection are definitely smaller (shifting the bracket from point A to point B in Fig.4).

Another option could be making small elongated holes on the A clasping block (see Fig.4) in order to compensate the flange deflection effect.

2. Stress Analysis

2.1 *Element description*

The model contains 7878 nodes and 6892 elements. The elements, listed in table 1 and 3, have been used to create the mesh of the tubes and the clasping blocks (see Fig.1).

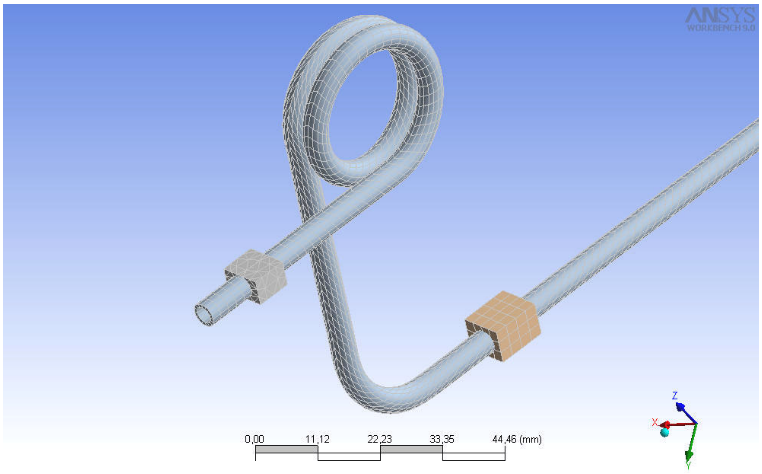

Fig. 1 – Mesh detail

General name	ANSYS element	Description
10-Node Quadratic Tetrahedron	Solid187	10-Node Tetrahedral Structural Solid
20-Node Quadratic Hexahedron	Solid186	20-Node Hexahedral Structural Solid
4-Node Linear Quadrilateral Shell	Shell181	4-Node Structural Shell

Tab.1 – Ansys elements used

To model the contacts between clasping blocks and tubes, the following elements and assumptions have been adopted:

Type	Associated Bodies	Scope	Normal Stiffness	Scope Mode	Formulation
Bonded	*Tube – internal clasping block*	Face, Face	Program Controlled	Symmetric	Pure Penalty
Bonded	*Tube – external clasping block*	Face, Face	Program Controlled	Symmetric	Pure Penalty
Bonded	*Tube – central clasping block*	Face, Face	Program Controlled	Symmetric	Pure Penalty

Tab.2 – Contact assumptions

General name	Name in ANSYS	Description
Quadratic Quadrilateral Contact	Conta174	Hi-order Surface to Surface Contact
Quadratic Triangular Contact	Conta174	Hi-order Surface to Surface Contact
Linear Quadrilateral Target	Targe170	Surface Contact Target

Tab.3 – Ansys elements used in the contact area

2.2 *Material properties*

In table 4 the properties of the material used for the tubes (CRES 316L) and for the clamps (AL 6082) are reported:

	AL 6082	CRES 316 L
Density	$2{,}77\times10^{-6}$ kg/mm³	7.85×10^{-6} kg/mm³
Poisson's Ratio	0,33	0.3
Tensile Yield Strength	240,0 MPa	319.0 MPa
Tensile Ultimate Strength	300,0 MPa	632.0 MPa
Young's Modulus	71.000,0 MPa	200,000.0 MPa

Tab.4 – Material properties

2.3 *Deflection of VC flange*

In the preceding FEM investigation (ASR-D-005), the evaporator section of the Tracker Thermal Control System (see Fig.2) has been analysed.

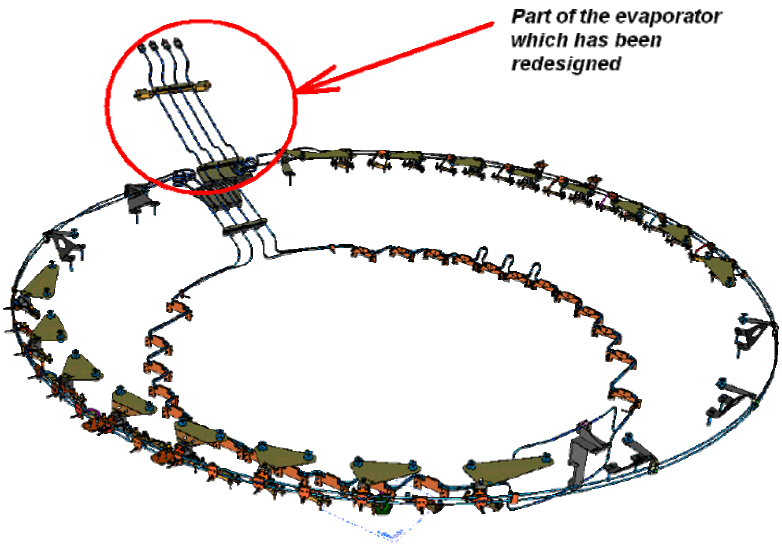

Fig. 2 – Previous layout overview

As it is explained in the section 6 of the aforementioned document, the vacuum case will be evacuated before the launch and, as a result, a deformation in a downwards direction (10mm at maximum) will occur for the protruding tubes (see Fig.3).

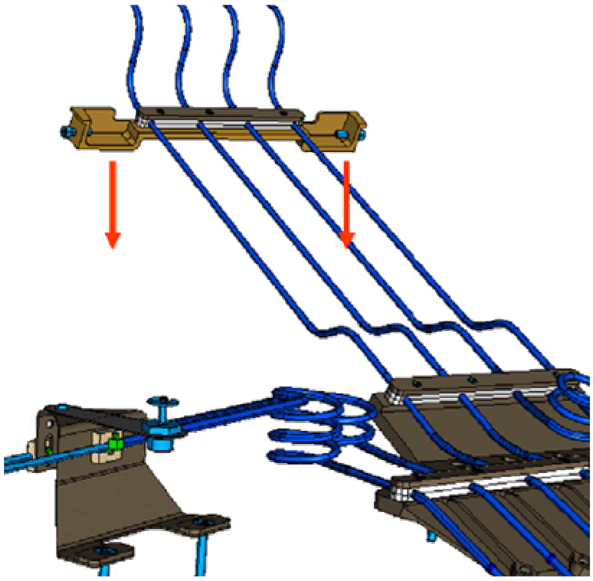

Fig. 3 – Deflection of the clasping bracket (previous design)

Based on the results of the structural analysis, the stress on the cooling pipes turned out to be too high (434Mpa). In addition, this deformation is present during launch and it has to be added to the acceleration stress. Consequently, it has been decided to modify the old lay out of the exit tubes in order to make it more flexible (see Fig.4).

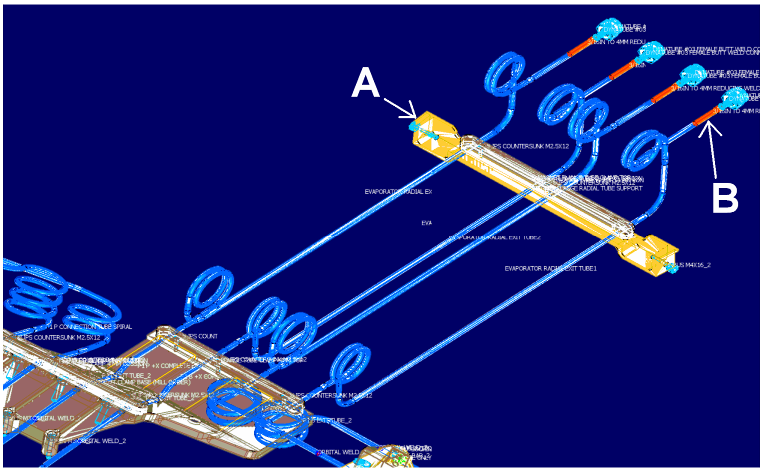

Fig. 4 – New design of the outgoing pipes with clasping blocks

The new design has been re-analyzed (using the ANSYS® engineering software program) in order to investigate both the maximum not-critical deflection and the minimum vibrational modes and the results are presented below.

2.3.1 *Loads and supports*

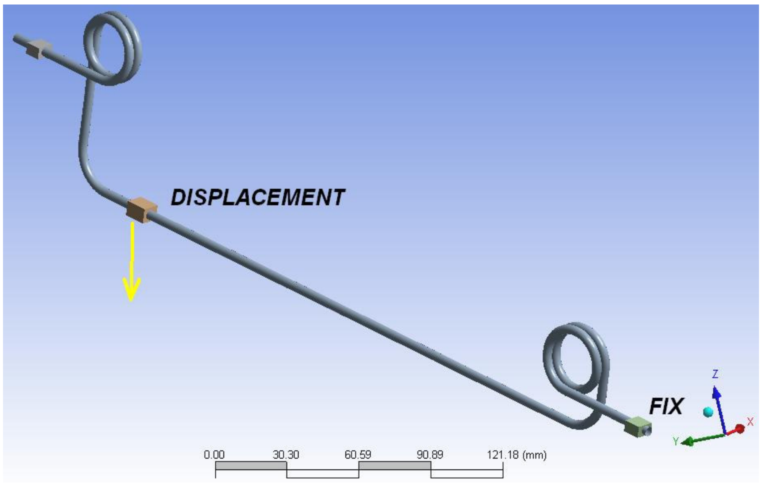

Fig.5 – Loads and supports for the stress analysis

2.3.2 *Results of the analysis*

2.3.2.1 Multi-scenario investigation

In order to get more information about the new design, several scenarios have been investigated. Each scenario presented below represents one complete engineering simulation. The results of a simulation provide insight into how the tubes may deflect without getting a negative Margin of Safety. Multiple scenarios allow comparison of results given different displacements.

The results of the stress calculation for several load condition can be seen in Tab.5. Units of the stress values in the plots are in N/mm^2. The highest Von Mises stresses occurs in the region of the central bracket (all the Margin of Safety (Tab.5) have been calculated with the factors shown in APPENDIX 3)

Run	Displacement of the clasping block (mm)	Max Von Mises Stress (MPa)	Minimum Yield MS	Minimum Ultimate MS
1	6.0	144.12	0,77	1.21
2	8.0	192.15	0,328	0.66
3	10.0	240.19	0,062	0.33
4	12.0	288.23	-0,11	0.11

Tab.5 – Stress and MS under several displacement

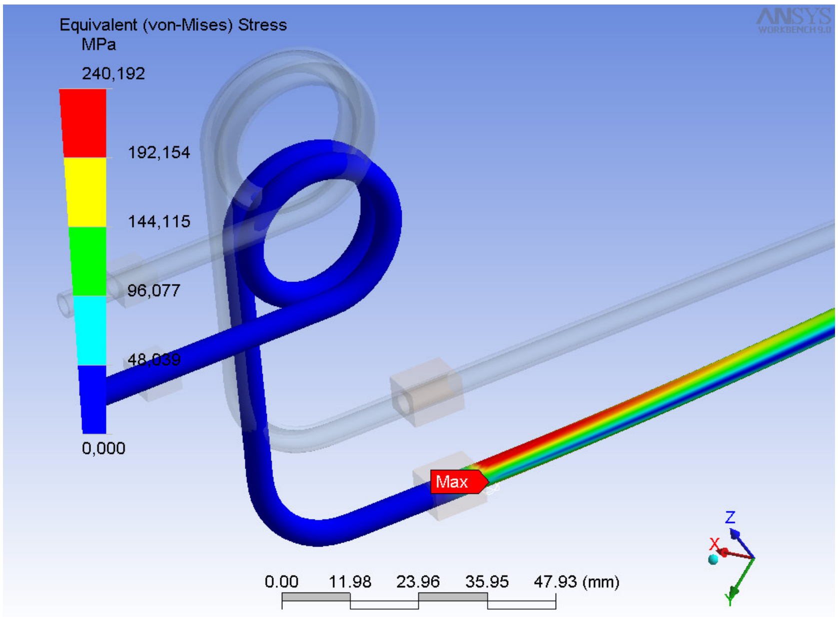

Fig.6 - Von Mises stress with a deflection of 10 mm (with un-deformed shape displayed)

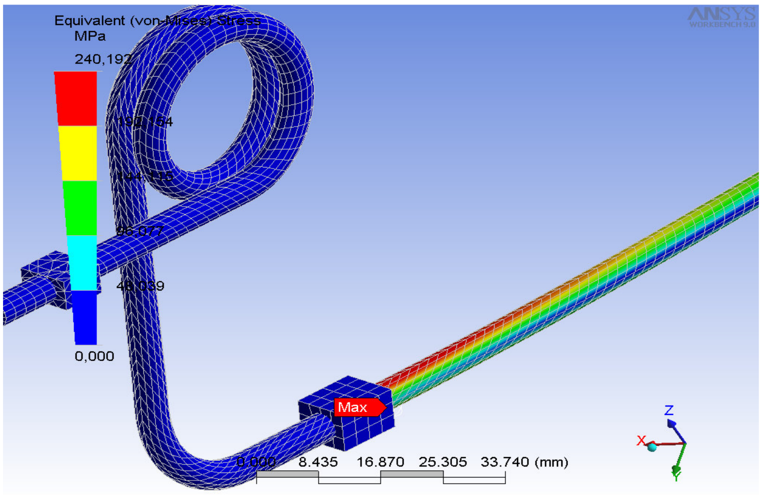

Fig.7 - Von Mises stress with a deflection of 10 mm – (Max: 240MPa)

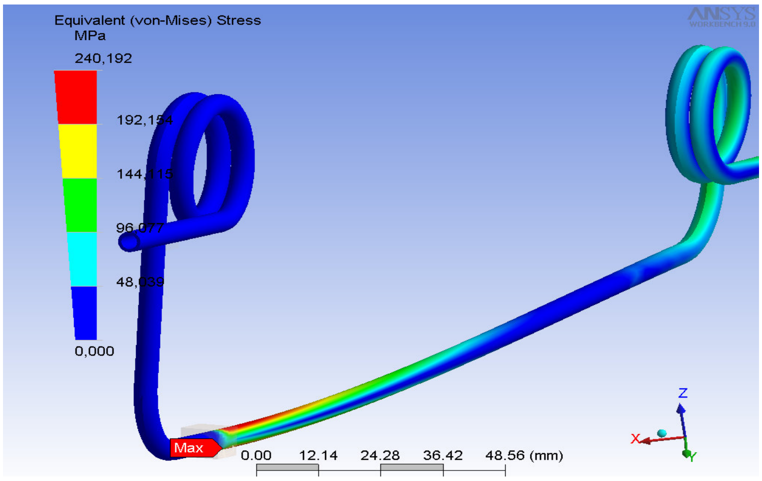

Fig.8 – V.Mises stress with a deflection of 10 mm only on the tube surface (Max.240MPa)

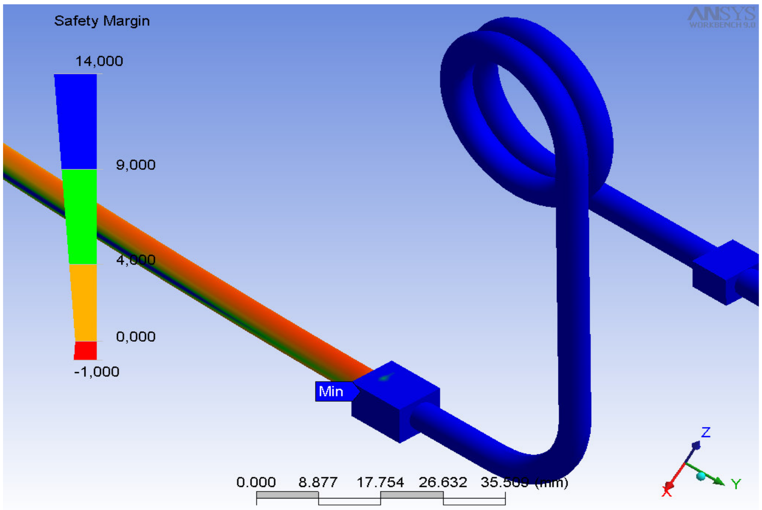

Fig.9 – Minimum Ultimate Margin of Safety: 0,33 (deflection of 10 mm)

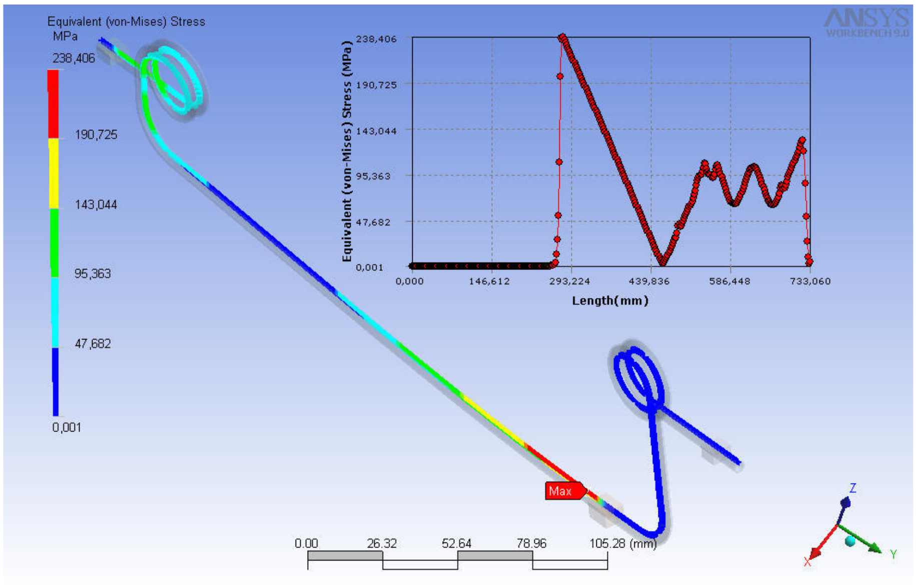

Fig.10 – V.Mises stress scoped along a line (deflection of 10 mm)

2.3.2.2 Stress analysis and convergence with a displacement of 10 mm

The multi-scenario analysis showed that a displacement of 10mm allows us to have a positive MS. Then a Convergence analysis has been performed for evaluating the quality of calculated results and the acceptability of the values (just considering a 10mm displacement). The *Solution history,* shown in Tab.7, provides a mean of assessing the quality of results by examining how values change during successive iterations of solution refinement. *Convergence criteria* sets a specific limit on the allowable change in a result between iterations (which has been set at 2% in this analysis).

Name	**Type**	**Allowable Change**	**Last Change**	**Status**
"Von Mises on the tube"	Maximum	± 2.0%	+0.76%	Converged

Tab.6 – Convergence Tracking

Name	**Base Solution**	**Refinement 1**	**Refinement 2**
Von Mises on the tube	240.19 MPa	245.31 MPa [+2.11%]	247.17 MPa [+0.76%]
Mesh properties	Nodes: 7878 Elements: 6892	Nodes: 8625 Elements: 7732	Nodes: 10490 Elements: 9695

Tab.7 – Solution History

As it is shown in the following pictures, the minimum ultimate MS is 0,33 and it occurs near the central clasping bracket:

Perugia INFN Istituto Nazionale di Fisica Nucleare

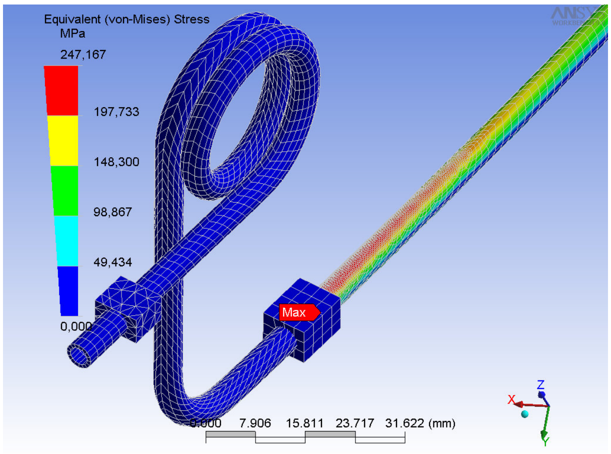

Fig.11 - Max V.Mises stress after refinement (10mm deflection)

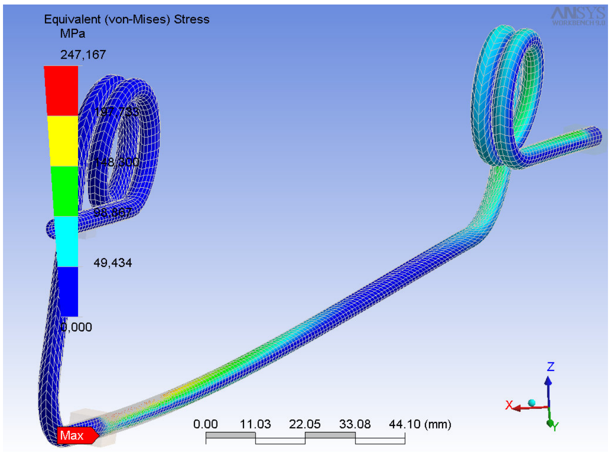

Fig.12 - Max V.Mises stress after refinement (10 mm deflection)

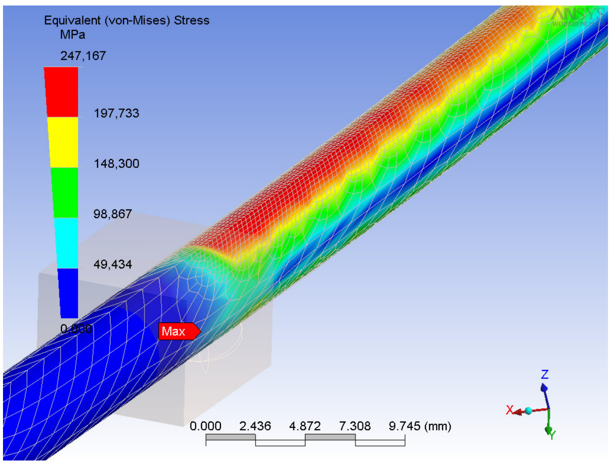

Fig.13 - Mesh has been refined just on the critical area with the maximum V.Mises stress.

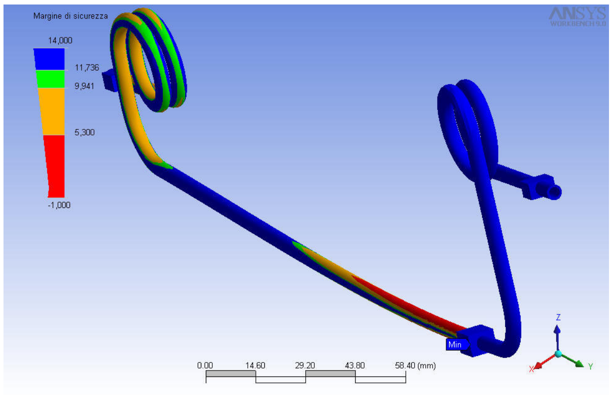

Fig.14 – The minimum ultimate MS (0,33) occurs near the central clasping bracket

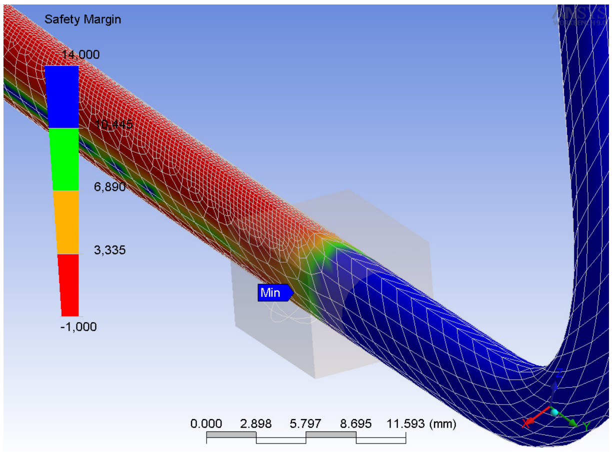

Fig.15 – Detail of the clasping block and refined mesh

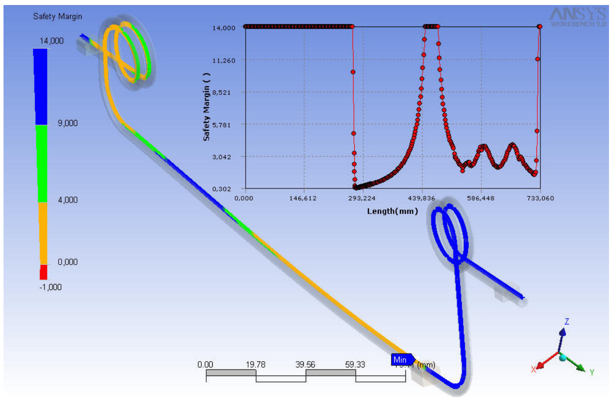

Fig.16 – MS variation along all the tube. Minimum Ultimate MS, after mesh refinement, is 0,29

2.4 *Relative displacement*

The coordinates of the points (in which the brackets of the evaporator pigtails are attached) are shown in Fig.17 on AMS reference system:

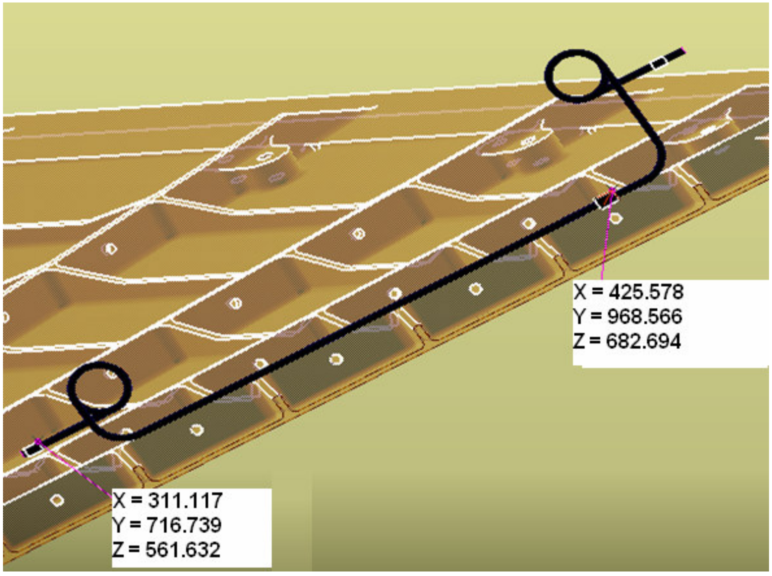

Fig. 17 – Bracket location in the upper flange

The displacements for the two grids on the Vacuum Case Conical Flange which are closest to the points indicated in fig.17 and to the symmetrical points on the bottom flange are defined in cylindrical coordinate system (radial, tangential, and vertical) in tab.8 and 9.

The displacements have been provided by Jacobs (see in the attached file “VC Flange Displacements for TTCS.xls”) which also mentioned the possibility that the real displacements could be larger given the fact that one end of the tube is attached to the Tracker Conical Flange (see Fig. 3) and the other to the Vacuum Case Flange. Since Jacobs doesn’t have the Tracker structure explicitly in the model (they account for the total mass of the Tracker by placing concentrated mass elements at the attachment locations of the Tracker to Vacuum Case interface) they suggested to make a design with enough flexibility to account for any additional deformations that may not be accounted for in the attached data (by leaving a large MS in the final design).

GRID locations UPPER Flange			
GRID ID	r (in)	Theta (deg)	z (in)
11596	42,0871	67,5	417,86
11692	31,3451	67,5	412,511

Tab.8 – Grid location UPPER Flange

GRID locations BOTTOM Flange			
GRID ID	r (in)	Theta (deg)	z (in)
13432	42,0871	67,5	366,734
13528	31,3451	67,5	372,083

Tab.9 – Grid location BOTTOM Flange

As it is shown in the attached file "VC Flange Displacements for TTCS.xls" , 128 load cases have been applied (1001 – 1064 and 2001 – 2064) and the results have been reported (in Cartesian coordinates) for each of those 4 points corresponding to the locations of the pigtails brackets.

Preventing to investigate again all the 512 load cases, only the worse (based on the maximum relative displacement between the 2 points) load cases have been selected so far.

The maximum relative displacement between clasping blocks has been calculated as the following example shows for the load case 1001:

given the displacement for the node 11596,

GRID ID	Load Case	Tr (in)	Ttheta (in)	Tz (in)
11596	1001	2,73E-01	-9,43E-02	-7,25E-02

and the one for the node 11692,

GRID ID	Load Case	Tr (in)	Ttheta (in)	Tz (in)
11692	1001	2,66E-01	-1,14E-01	-5,87E-02

the **relative displacement** of node 11596 respect to 11692 is:

Load Case	ΔTr (in)	ΔTtheta (in)	ΔTz (in)
1001	(2,73E-01) – (2,66E– 01)	– 9,43E–02 – (–1,14E–01)	– 7,25E– 02 – (–5,87E– 02)

Then, the **modulus** of the relative displacement vector is:

$$\sqrt{(\Delta Tr)^2 + (\Delta Ttheta)^2 + (\Delta Tz)^2}$$

2.4.1 Loads and supports

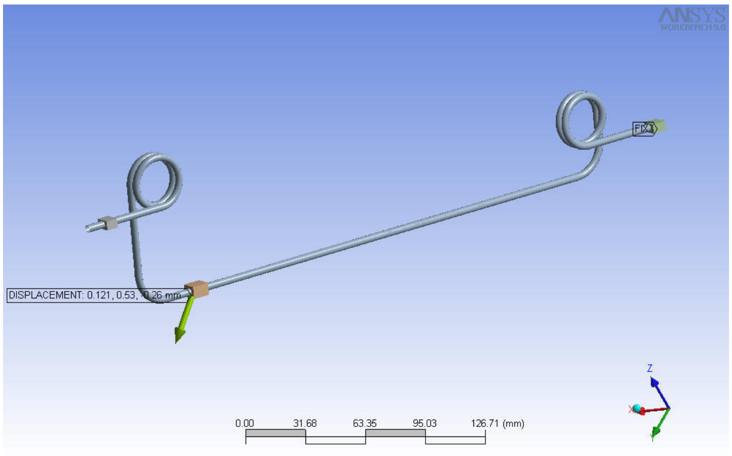

Fig.18 – Loads and supports for - load case 1024

2.4.2 Results of the analysis

In Tab.10 the Von Mises Stress and the minimum MS have been listed for the 15 largest relative displacements. The worse load case between those seems to be number 1011

Run	X – Displacement (mm)	Y – Displacement (mm)	Z – Displacement (mm)	Von Mises (MPa)	MS	LOAD CASE
1	0.13	0.63	-0.28	73.71	3.33	1007
2	0.13	0.63	-0.27	73.52	3.34	1003
3	0.15	0.59	-0.32	67.15	3.75	1008
4	0.15	0.59	-0.3	67.88	3.7	1004
5	0.11	0.63	-0.23	74.98	3.25	1015
6	**0.1**	**0.63**	**-0.22**	**75.83**	**3.21**	**1011**
7	0.13	0.59	-0.27	68.62	3.65	1016
8	0.12	0.58	-0.25	68.78	3.64	1012
9	0.16	0.49	-0.36	54.86	4.81	1005
10	0.15	0.54	-0.31	61.48	4.19	1023
11	0.18	0.45	-0.29	53.84	4.92	1006
12	0.16	0.49	-0.38	53.28	4.99	1001
13	0.18	0.54	-0.33	62.13	4.13	1019
14	0.16	0.49	-0.33	55.69	4.73	1002
15	0.12	0.53	-0.26	61.19	4.21	1024

Tab.10 – Results of the analysis for different load cases

The following graph (Fig. 19) shows the general decreasing trend of the Von Mises stress according to the declining of the relative displacement (no matter which is the direction of the vector).

As a result, and given the time available, I assumed that the most critical load case is included in the first 15 biggest displacement.

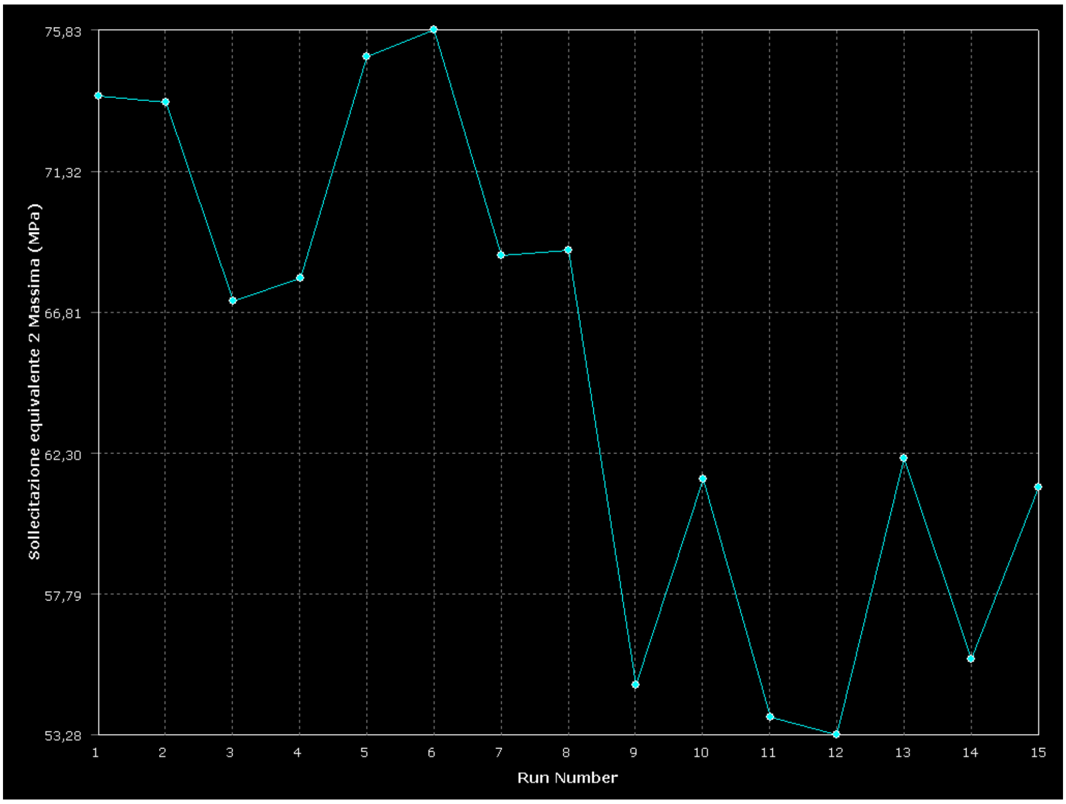

Fig. 19 – Von Mises VS run number

2.5 *Internal pressure*

Based on ICD thermal profile, the expected cargo bay temperature at launch is 48,9 C° then, being the internal pressure of the fluid dependent on the temperature (the maximum is 160 bar at 60'C), 160 bar have been applied to be conservative.

Both formulas and FEM simulation have been used to show that the internal pressure during launch/abort landing would be negligible relative to the operational pressure or burst pressure of the tubes.

2.5.1 Design by formulas

The code applied to calculate the stress resulting from the internal pressure is **ASME B-31.3 – 2002** for the **Curved Segments of Pipe (304.2.1)**. The minimum required thickness t_m ($t_m = t + c$) of a bend, after bending, in its finished form, shall be determined in accordance with the following equation:

$$t = \frac{PD}{2[(SE/I) + PY]} \tag{1}$$

where, at the intrados (inside bend radius)

$$I_{int} = \frac{4(R_1/D) - 1}{4(R_1/D) - 2} \tag{2}$$

And, at the extrados (outside bend radius)

$$I_{ext} = \frac{4(R_1/D) + 1}{4(R_1/D) + 2} \tag{3}$$

ASME B31.3-2002

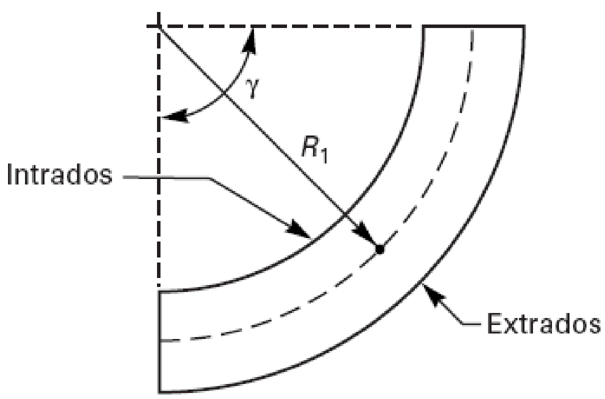

Then, by adjusting the previous formula:

$$S = \frac{(PD - 2tPY)I}{2tE} \tag{4}$$

where :

t = pipe wall thickness = 0,7mm
d = inside diameter of pipe = 2,6mm
P = internal design gage pressure =160 bar = 16,2 MPa
D = outside diameter of pipe = 4mm
E = quality factor from Table A -1A or A -1B (see APPENDIX 4) = 0,85
S = stress value
c = the sum of the mechanical allowances plus corrosion and erosion allowances = 0,05mm

$$\mathrm{Y} = \frac{d+2c}{D+d+2c} = \frac{2.6+2\cdot 0.05}{4+2.6+2\cdot 0.05} = 0.4 \quad \text{for } t > D/6 \tag{5}$$

According to our geometry (considering a R_1 = 13,25mm, TBC with Bart) we get:

$$I_{\text{int}} = 11.088$$
$$I_{ext} = 0.934$$

which substituted in (4):

$$S_{\text{int}rados} = \frac{(16.2\cdot 4 - 2\cdot 0.7\cdot 16.2\cdot 0.4)\cdot 1.088}{2\cdot 0.7\cdot 0.85} = 50.95MPa$$

$$S_{extrados} = \frac{(16.2\cdot 4 - 2\cdot 0.7\cdot 16.2\cdot 0.4)\cdot 0.934}{2\cdot 0.7\cdot 0.85} = 43.7MPa$$

2.5.2 Design by analysis

A FEM simulation has been made in order to verify the results gotten by formulas. The results by simulation confirmed the ones found by formulas. In fact, the max stress on the tube is 51,93MPa and the MAX deformation is about 0,02 mm. The tubes has been simply supported on both the external sides.

As it is shown in Tab 11, the MS are pretty high since the tubes has been correctly designed to withstand to a pressure much bigger than the operative one.

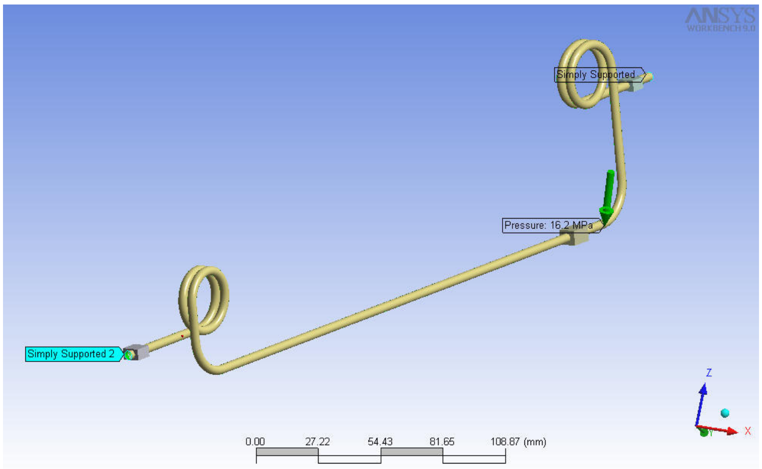

Fig. 20 – The only external load applied here is internal pressure (160 bar)

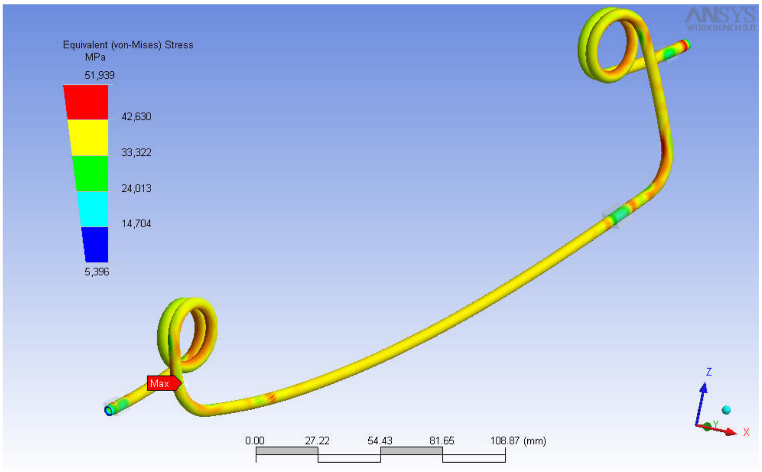

Fig. 21 – The maximum Von Mises stress in the tube is 51MPa.

Max Von Mises Stress (MPa)	Minimum Yield MS	Minimum Ultimate MS
51	4	5,19

Tab. 11 – Results of the analysis

2.6 *Loads combination*

2.6.1 Relative displacements and internal pressure

2.6.1.1 Loads and supports

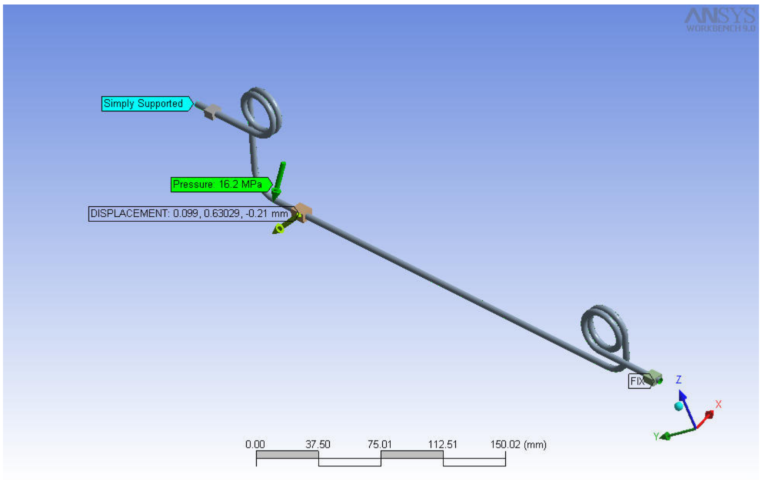

Fig.22 – Loads and supports

2.6.1.2 Results of the analysis

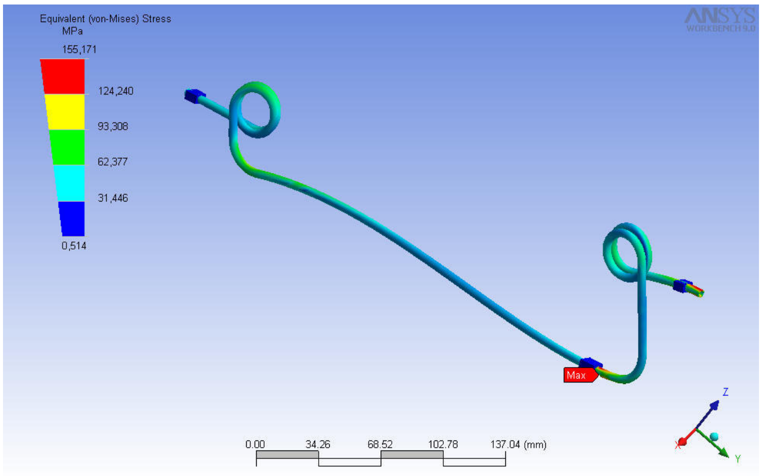

Fig.23 – Von Mises stress, Max stress:155,17MPa

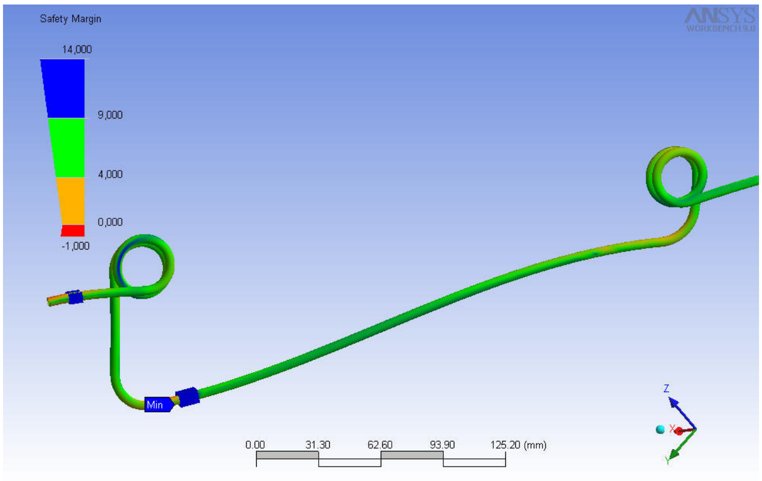

Fig.24 – Margin of Safety, Min MS = 1,06

Max Von Mises Stress (MPa)	Minimum Yield MS	Minimum Ultimate MS
155,17	0,64	1,04

Tab. 12 – Margins of Safety

2.6.2 Relative displacements, internal pressure and VC flange deflection

2.6.2.1 Loads and supports

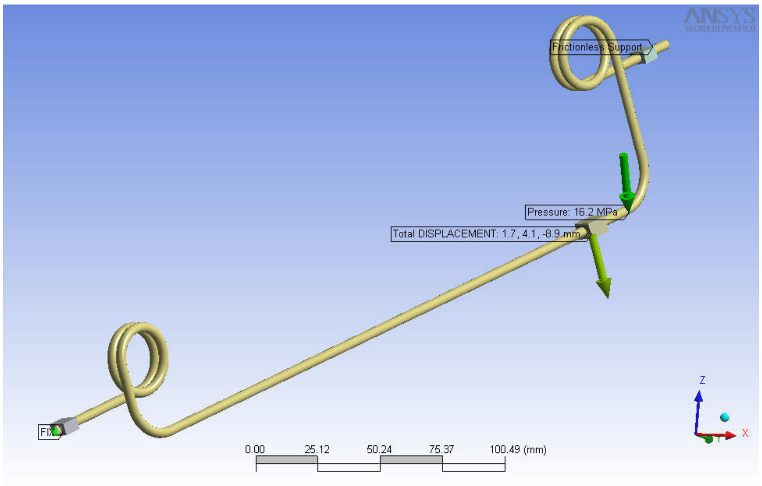

Fig.25 – Loads and supports

2.6.2.2 Results of the analysis

In order to combine the displacement loads (due both to the VC deflection and to the launch loads), the VC deformation vector has been expressed in the global AMS reference system. In Tab. 13 there is the relative position of one system respect to the other.

Name	Type	Origin (mm)	X Axis	Y Axis	Z Axis
AMS reference system	Cartesian	0.0, 0.0, 0.0	1.0, 0.0, 0.0	0.0, 1.0, 0.0	0.0, 0.0, 1.0
Local coordinate system	Cartesian	422.74, 961.71, 675.23	0.98, -7.36×10^{-2}, 0.16	0.0, -0.91, -0.42	0.17, 0.42, -0.89

Tab. 13 – Coordinate Systems

X Displacement (mm)	Y Displacement (mm)	Z Displacement (mm)	Von Mises (MPa)	Minimum Yield MS	Minimum Ultimate MS	Comments
1.79	4.73	-9.1	357.28	-0.28	-0.11	10mm VC DEFORMATION
1.45	3.91	-7.34	295.89	-0.13	0.07	8mm VC DEFORMATION
1.1	3.0	-5.56	229.13	0.11	0.38	6mm VC DEFORMATION
0.77	2.27	-3.78	192.6	0.33	0.64	4mm VC DEFORMATION

Tab. 14 – Results of the analysis **with all three kinds of load acting together**

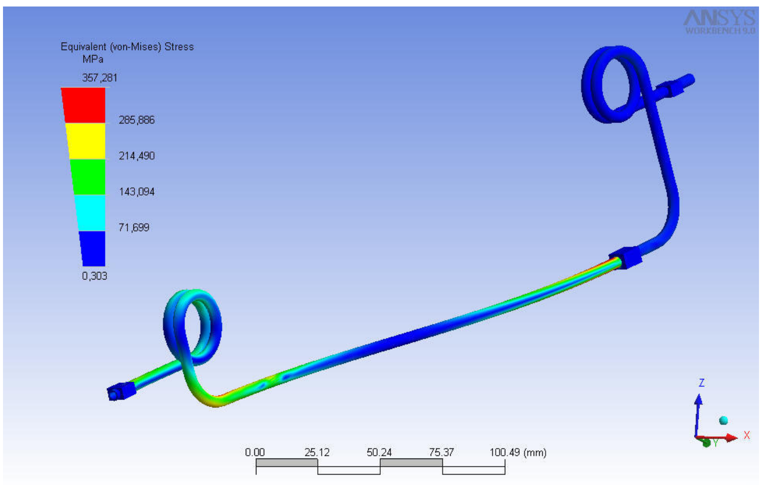

Fig. 26 – Max Von Mises Stress with a VC deformation of 10mm = 357MPa

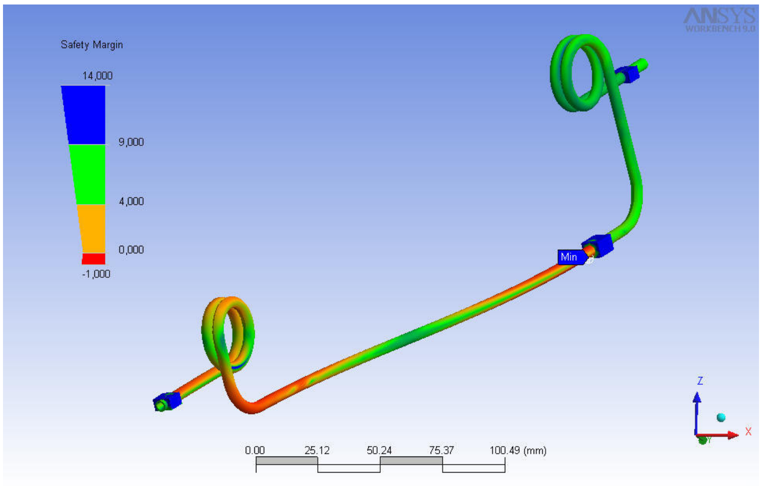

Fig.27 – Minimum yield MS (with 10mm VC deformation) is – 0.28

3. Frequency Analysis

In fig.28 the local loads and supports are illustrated .

3.1.1 Structural Supports

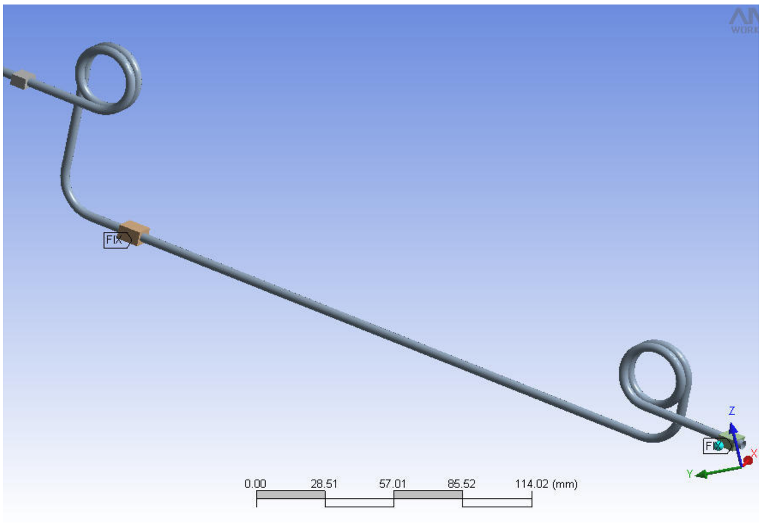

Fig.28 – Structural supports overview (2 fixed surfaces have been considered)

3.1.2 Frequency Results

The first 6 frequencies have been listed in the tab.15. Actually, since the system will be constrained on the connector side as well, the only interesting resonant mode for us is the 3rd one which occurs at 219Hz. However, it is good to note that the first mode is > 50 Hz even if the tubes are completely unconstrained at one side (and this is conservative). In Appendix 1, all the 6 resonant mode shapes have been reported anyway.

Name	Frequency
1º MODE	148.95 Hz
2º MODE	157.86 Hz
3º MODE	**217.65 Hz**
4º MODE	266.9 Hz
5º MODE	288.93 Hz
6º MODE	309.82 Hz

Tab.15 – MODE FREQUENCIES

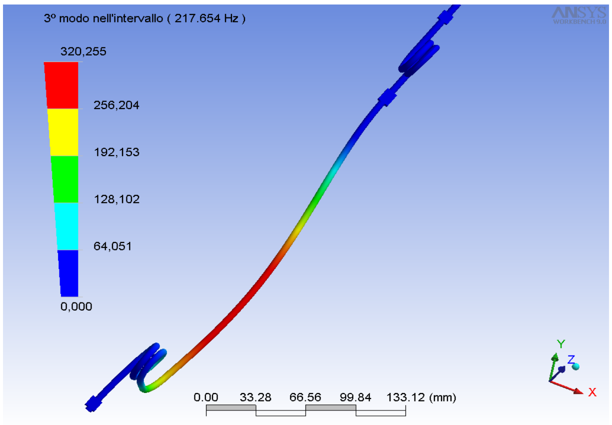

Fig.29 – Third mode: 217 Hz

APPENDIX 1: Frequency analysis (Mode shapes)

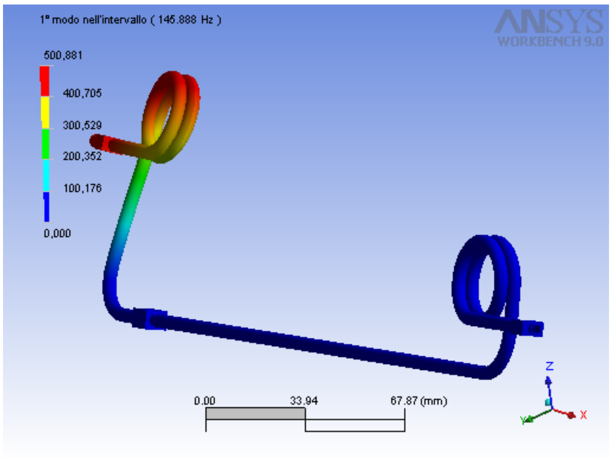

First mode: 146 Hz

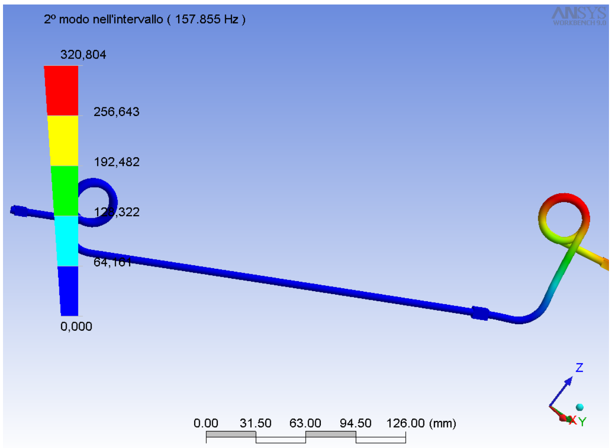

Second mode: 157 Hz

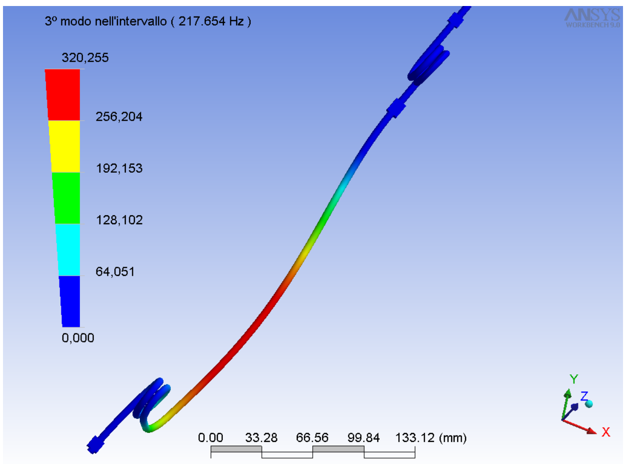

Third mode: 217 Hz

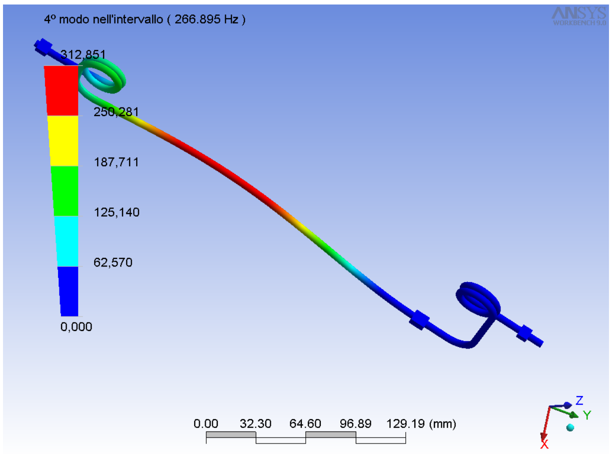

Fourth mode: 267 Hz

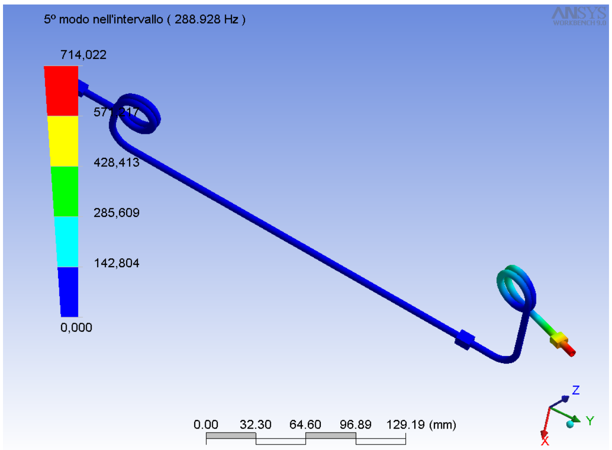

Fifth mode: 289 Hz

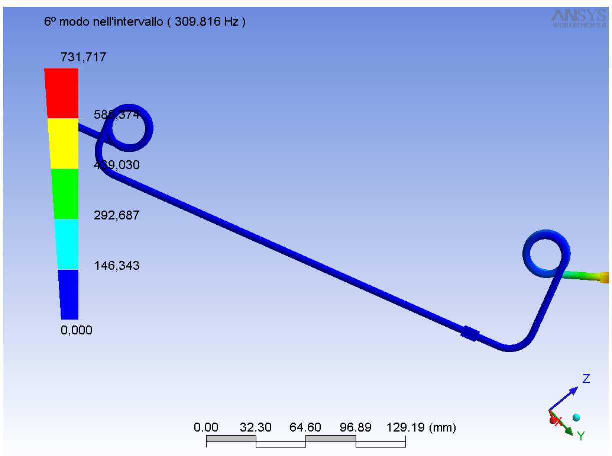

Sixth mode: 309 Hz

APPENDIX 2: New mechanical design

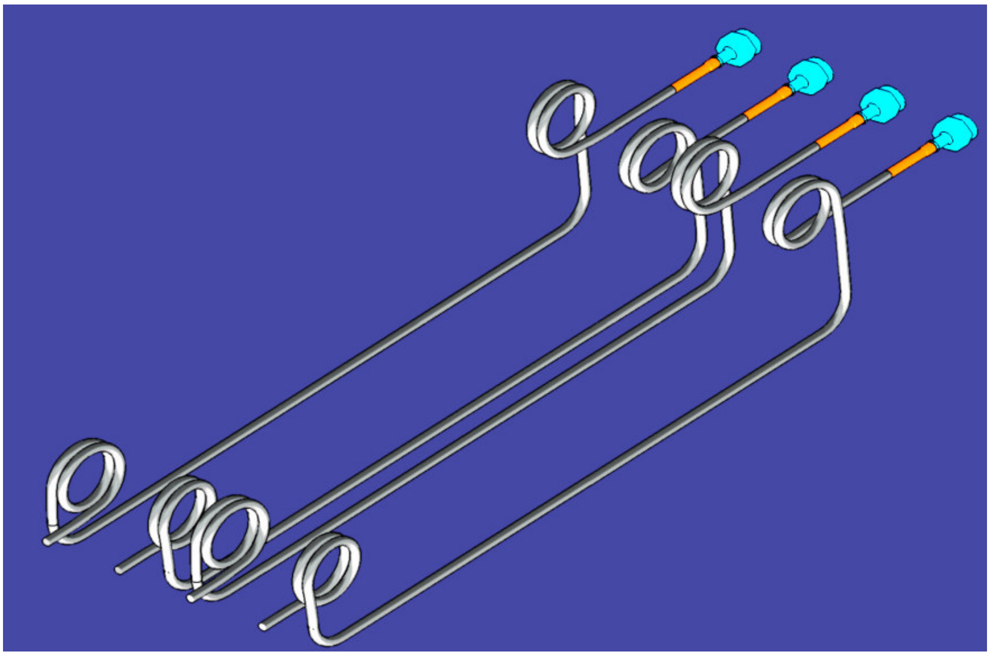

APPENDIX 3: Safety factors

The safety factor for yield must be 1.25, the ultimate safety factor must be 2. The Margin of Safety, has to be calculated as follows:

$$MSy = \frac{FTy}{FSy * f} - 1 \qquad MSu = \frac{FTu}{FSu * f} - 1$$

MSx=Margin of safety for yield or ultimate
FSx=Factor of safety for yield or ultimate
FTx=Ultimate or Yield stress
f=Maximum limit stress
u=ultimate
y=yield

APPENDIX 4: Basic Casting Quality Factor (ASME B31.3 – 2002)

These quality factors are determined in accordance with para. 302.3.3(b). See also para. 302.3.3(c) and Table 302.3.3C for increased quality factors applicable in special cases. Specifications are ASTM.

Spec. No.	Description	E_c (2)	Appendix A Notes
Iron			
A 47	Malleable iron castings	1.00	(9)
A 48	Gray iron castings	1.00	(9)
A 126	Gray iron castings	1.00	(9)
A 197	Cupola malleable iron castings	1.00	(9)
A 278	Gray iron castings	1.00	(9)
A 395	Ductile and ferritic ductile iron castings	0.80	(9)(40)
A 571	Austenitic ductile iron castings	0.80	(9)(40)
Carbon Steel			
A 216	Carbon steel castings	0.80	(9)(40)
A 352	Ferritic steel castings	0.80	(9)(40)
Low and Intermediate Alloy Steel			
A 217	Martensitic stainless and alloy castings	0.80	(9)(40)
A 352	Ferritic steel castings	0.80	(9)(40)
A 426	Centrifugally cast pipe	1.00	(10)
Stainless Steel			
A 351	Austenitic steel castings	0.80	(9)(40)
A 451	Centrifugally cast pipe	0.90	(10)(40)
A 487	Steel castings	0.80	(9)(40)
Copper and Copper Alloy			
B 61	Steam bronze castings	0.80	(9)(40)
B 62	Composition bronze castings	0.80	(9)(40)
B 148	Al-Bronze and Si-Al-Bronze castings	0.80	(9)(40)
B 584	Copper alloy castings	0.80	(9)(40)
Nickel and Nickel Alloy			
A 494	Nickel and nickel alloy castings	0.80	(9)(40)
Aluminum Alloy			
B 26, Temper F	Aluminum alloy castings	1.00	(9)(10)
B 26, Temper T6, T71	Aluminum alloy castings	0.80	(9)(40)